

AD

TECHNICAL REPORT ARCCB-TR-00001

**EROSION EFC FACTORS FOR KINETIC ENERGY
ROUNDS USED IN THE 120-MM M256 TANK CANNON**

**SAMUEL SOPOK
ROGER BILLINGTON**

JANUARY 2000



**US ARMY ARMAMENT RESEARCH,
DEVELOPMENT AND ENGINEERING CENTER
CLOSE COMBAT ARMAMENTS CENTER
BENÉT LABORATORIES
WATERVLIET, N.Y. 12189-4050**



APPROVED FOR PUBLIC RELEASE; DISTRIBUTION UNLIMITED

DTIC QUALITY INSPECTED 4

20000201 024

DISCLAIMER

The findings in this report are not to be construed as an official Department of the Army position unless so designated by other authorized documents.

The use of trade name(s) and/or manufacturer(s) does not constitute an official endorsement or approval.

DESTRUCTION NOTICE

For classified documents, follow the procedures in DoD 5200.22-M, Industrial Security Manual, Section II-19, or DoD 5200.1-R, Information Security Program Regulation, Chapter IX.

For unclassified, limited documents, destroy by any method that will prevent disclosure of contents or reconstruction of the document.

For unclassified, unlimited documents, destroy when the report is no longer needed. Do not return it to the originator.

REPORT DOCUMENTATION PAGE			Form Approved OMB No. 0704-0188	
Public reporting burden for this collection of information is estimated to average 1 hour per response, including the time for reviewing instructions, searching existing data sources, gathering and maintaining the data needed, and completing and reviewing the collection of information. Send comments regarding this burden estimate or any other aspect of this collection of information, including suggestions for reducing this burden, to Washington Headquarters Services, Directorate for Information Operations and Reports, 1215 Jefferson Davis Highway, Suite 1204, Arlington, VA 22202-4302, and to the Office of Management and Budget, Paperwork Reduction Project (0704-0188), Washington, DC 20503.				
1. AGENCY USE ONLY (Leave blank)	2. REPORT DATE January 2000	3. REPORT TYPE AND DATES COVERED Final		
4. TITLE AND SUBTITLE EROSION EFC FACTORS FOR KINETIC ENERGY ROUNDS USED IN THE 120-MM M256 TANK CANNON			5. FUNDING NUMBERS PRON No. J5850E52M21A	
6. AUTHOR(S) Samuel Sopok and Roger Billington (PM-TMAS, Picatinny Arsenal, NJ 07806)				
7. PERFORMING ORGANIZATION NAME(S) AND ADDRESS(ES) U.S. Army ARDEC Benet Laboratories, AMSTA-AR-CCB-O Watervliet, NY 12189-4050			8. PERFORMING ORGANIZATION REPORT NUMBER ARCCB-TR-00001	
9. SPONSORING / MONITORING AGENCY NAME(S) AND ADDRESS(ES) U.S. Army ARDEC Close Combat Armaments Center Picatinny Arsenal, NJ 07806-5000			10. SPONSORING / MONITORING AGENCY REPORT NUMBER	
11. SUPPLEMENTARY NOTES Presented at the 35 th AIAA Joint Propulsion Conference, Los Angeles, CA, 20-24 June 1999. Published in proceedings of the conference.				
12a. DISTRIBUTION / AVAILABILITY STATEMENT Approved for public release; distribution unlimited.			12b. DISTRIBUTION CODE	
13. ABSTRACT (Maximum 200 words) The U.S. Army and Air Force's standard manual for the evaluation of cannon tubes designates fatigue condemnation criteria for each cannon tube type. It also designates erosion condemnation criteria for each cannon tube type, and designates a cartridge/zone fatigue effective full charge (EFC) factor for each charge/projectile combination. These criteria help in cannon inventory management. However, the manual lacks a designated cartridge/zone erosion EFC factor for each charge/projectile combination. This represents a notable technology gap for tank and artillery cannon systems, since erosion condemnation occurs much quicker than fatigue condemnation when using the latest charge/projectile combinations. Our report outlines a detailed computational and experimental method using the Unified Cannon Erosion Code to compute a cartridge or round erosion EFC factor for the M865, M829, M829A1, and M829A2 kinetic energy round types used in the 120-mm M256 tank cannon at multiple round-conditioning temperatures. Our report further outlines the obvious extension of this method to any group of charge/projectile combinations used in a specific tank or artillery cannon. The following erosion EFC factors are based on an erosion EFC factor of 1.0 for the M865 round type at a 21°C round-conditioning temperature as requested by PM-TMAS. These erosion factors correspond to a peak erosion location approximately 2.2 meters from the rear face of the tube. For the M865, M829, M829A1, and M829A2 round types at a 49°C round-conditioning temperature, the respective erosion EFC factors are approximately 1.5, 4.2, 5.0, and 6.3. Similarly, the respective erosion EFC factors are approximately 1.0, 2.8, 3.3, and 4.2 at a 21°C round-conditioning temperature, and the respective erosion EFC factors are approximately 0.7, 1.9, 2.2, and 2.8 at a -32°C round-conditioning temperature. The respective erosion EFC factors are approximately 1.1, 3.0, 3.5, and 4.4 for an equal distribution of these three round-conditioning temperatures. M256 cannon fatigue life and fatigue EFC factors are officially specified in the above technical manual and help the Army manage its M256 inventory. They are not round type or conditioning temperature-dependent. M256 cannon erosion life and erosion EFC factors are unofficially specified in this work, and will further help the Army manage its M256 inventory. They are both round type and conditioning temperature-dependent. M256 cannon erosion-related inventory management is important, since its erosion life can be up to an order of magnitude more limiting than its associated fatigue life.				
14. SUBJECT TERMS Gun Barrel Erosion, Kinetic Energy Round EFC Factors, Kinetic Energy Round Erosion, 120-mm M256 Tank Cannons			15. NUMBER OF PAGES 18	
			16. PRICE CODE	
17. SECURITY CLASSIFICATION OF REPORT UNCLASSIFIED	18. SECURITY CLASSIFICATION OF THIS PAGE UNCLASSIFIED	19. SECURITY CLASSIFICATION OF ABSTRACT UNCLASSIFIED	20. LIMITATION OF ABSTRACT UL	

TABLE OF CONTENTS

	<u>Page</u>
INTRODUCTION	1
COMPUTATIONAL AND EXPERIMENTAL METHODS	2
RESULTS AND DISCUSSION.....	3
REFERENCES	8

LIST OF ILLUSTRATIONS

1.	M256 calibrated XNOVAKTC interior ballistics analysis for maximum values of gas pressure	9
2.	M256 calibrated XNOVAKTC interior ballistics analysis for maximum values of gas temperature	9
3.	M256 calibrated XNOVAKTC interior ballistics analysis for maximum values of gas velocity	10
4.	M256 calibrated MABL analysis for maximum values of recovery enthalpy	10
5.	M256 calibrated MABL analysis for maximum values of cold wall heat flux	11
6.	M256 calibrated CCET thermochemical analysis for respective values of mean reacting wall enthalpy and mean ablation potential.....	11
7.	Borescope analysis of the A723 subsurface exposure.....	12
8.	M256 calibrated MACE wall temperature profile analysis for maximum values of HC chromium surface temperature.....	12
9.	M256 calibrated MACE wall temperature profile analysis for maximum values of A723 interface temperature	13
10.	M256 calibrated MACE wall temperature profile analysis for maximum values of A723 surface temperature	13
11.	M256 MACE analysis of rounds-to-gas wash onset and rounds-to-erosion condemnation for round-conditioning temperature of 49°C	14
12.	M256 MACE analysis of rounds-to-gas wash onset and rounds-to-erosion condemnation for round-conditioning temperature of 21°C	14

13.	M256 MACE analysis of rounds-to-gas wash onset and rounds-to-erosion condemnation for round-conditioning temperature of -32°C.....	15
14.	M256 MACE analysis of rounds-to-gas wash onset and rounds-to-erosion condemnation for an equal distribution of 49°C, 21°C, and -32°C	15
15.	M256 MACE erosion EFC analysis based on an erosion EFC factor of 1.0 for the M865 round type at 21°C round-conditioning temperature.....	16

INTRODUCTION

The U.S. Departments of Army and Air Force jointly publish a technical manual for the evaluation of cannon tubes (ref 1). The first paragraph of this manual states,

"The purpose of this manual is to aid you in determining if a cannon tube can continue to be used or condemned, in estimating the remaining life, and in determining how often a new tube can be installed into the breech ring or breech coupling. You will find information in this manual on tube life, erosion (wear), damage, and inspection procedures which will be helpful in making the right decision."

For each type classified cannon, this manual and its appendices give associated safe service life or fatigue life condemnation criteria, which designate the maximum number of effective full charge (EFC) rounds that can be fired before the cannon is condemned. Cracks or other damage may limit this maximum number as the manual quantitatively indicates. These values are based on strict methods (laboratory simulation, live fire, and modeling) dictated by the Army's Test and Evaluation Command for each type classified cannon's highest maximum pressure type classified charge/projectile combination. Safe service life values are very conservative and are known to have a high degree of confidence in order to reduce the chances of a catastrophic failure. The safe service life value of the 120-mm M256 tank cannon is 1500 EFC rounds.

For each type classified charge/projectile combination, this manual and its appendices give an associated cartridge or zone EFC factor, which is officially an accumulating standardized fatigue life factor. These values are based on strict methods (laboratory simulation, live fire, and modeling) dictated by the Army's Test and Evaluation Command for each type classified cannon and associated charge/projectile combination. Large caliber tank and medium caliber direct-fire cannons typically incorporate this charge/projectile combination into a single cartridge. All direct-fire rounds typically have an EFC factor of one, regardless of whether their highest or lowest maximum pressure round type is fired. In fact, the following round types for the 120-mm M256 tank have an EFC factor of one, including its advanced M829A2 kinetic energy (KE) round, its previous M829A1 KE round, its initial M829 KE round, and its M865 KE trainer round. This fatigue EFC factor in combination with the safe service life helps the Army manage its M256 inventory. Large caliber artillery, indirect-fire cannons typically incorporate this charge/projectile combination into single-to-multiple charge and single-projectile components. For a typical large caliber artillery cannon firing a single-charge/projectile combination, increasing the number of charges or zones, increases its associated EFC factor. For a typical artillery cannon firing a mix of charge/projectile combinations at the same zone, combinations that have a higher maximum pressure will have a higher associated EFC factor. It is interesting that round-conditioning temperature and firing rate are excluded from the fatigue life evaluation for tank and artillery cannon systems.

For each type classified cannon, the above manual and its appendices also give associated erosion life condemnation criteria, which designate a maximum allowable erosion depth at any bore surface location as measured by a bore erosion gauge. These values are based on strict

methods (live fire and modeling) dictated by the Army's Test and Evaluation Command for each type classified cannon's highest maximum pressure type classified charge/projectile combination. This erosion life condemnation depth is less critical than its fatigue counterpart above with a noncatastrophic, but important gas blow-by failure affecting target accuracy and precision. The erosion life condemnation depth of the 120-mm M256 tank cannon is 5-mm at any bore location. For each type classified charge/projectile combination used in its associated cannon, the above manual, its appendices, and the open literature do not provide a corresponding cartridge or zone erosion EFC factor. Since erosion condemnation occurs much quicker than fatigue condemnation in the latest type classified cannon systems, the lack of cartridge or zone erosion EFC factors represents a notable technology gap for tank and artillery cannon systems with a mixture of charge/projectile combinations, round-conditioning temperatures, and firing rates.

The general objective of this report is to outline a method for computing cartridge or zone erosion EFC factors, which unofficially represent an accumulating standardized erosion life factor for each type classified charge/projectile combination used in its associated cannon. The specific objective of this report is to outline a method in detail for computing a cartridge or round erosion EFC factor for the multiple KE round types used in the 120-mm M256 tank cannon. These erosion EFC factors, in combination with the erosion condemnation depth, will further help the Army manage its M256 inventory.

COMPUTATIONAL AND EXPERIMENTAL METHODS

The Unified Cannon Erosion Code is comprised of a collection of codes for predicting thermal-chemical-mechanical erosion in cannons. This collection of codes is used here to analyze interior ballistics, boundary layer, thermochemistry, and thermal and erosion characteristics for the 120-mm M256 cannon and its advanced M829A2 KE round, its previous M829A1 KE round, its initial M829 KE round, and its M865 KE trainer round. Selected round-conditioning temperatures include 49°C, 21°C, and -32°C, while selected axial positions from the rear face of the tube (RFT) include 0.7, 1.6, 2.2, 3.3, and 5.1 meters. Experimental data are used to guide and calibrate these nonlinear analyses. Two previous papers by this author (refs 2,3) provide a detailed description and the latest improvements of the Unified Cannon Erosion Code, which, in turn, consists of the following interactive codes.

- Standard interior ballistics gun code (XNOVAKTC)
- Standard heat transfer modified by mass addition to boundary layer rocket code modified for guns (MABL)
- Standard nonideal gas/wall thermochemical rocket code modified for guns (CCET)
- Standard wall material ablation conduction erosion rocket code modified for guns (MACE)

The XNOVAKTC interior ballistics code (refs 2-4) calculates the time-dependent core flow field characteristics for the 17.3-foot, 120-mm M256 cannon and its four M829A2/JA2, M829A1/JA2, M829/JA2, and M865/M14 round and propellant combinations. The "hotter" JA2 propellant consists of approximately 59% nitrocellulose, 15% nitroglycerine, 25% diethylene glycol dinitrate, and 1% other minor species, while the "cooler" M14 propellant consists of approximately 88% nitrocellulose, 8% dinitrotoluene, 2% butyl phthalate, 1% diphenylamine, and 1% other minor species. This interior ballistics analysis interacts with the boundary layer analysis (provides flow field/edge properties and state variable ranges) and thermochemistry analysis (receives propellant properties, provides state variable ranges). Validation of this code is based on its calibration with actual pressure gauge and radar data.

The MABL cannon code (refs 2,3) is based on previous rocket codes (refs 5,6) and calculates boundary layer characteristics for the above interior ballistics cases. This boundary layer analysis interacts with the interior ballistics analysis (receives flow field/edge properties and state variable ranges), thermochemistry analysis (receives chemical composition, compressibility, and transport properties), and thermal/erosion analysis (provides adiabatic recovery enthalpies, cold wall heat transfer rates, and edge pressures). Validation of this code is based on its calibration with actual subsurface metallographic data (recrystallization, reaction, and transformation depths) and thermocouple data.

The CCET cannon code (refs 2,3,7) is based on previous rocket and cannon codes (refs 8,9) and calculates gas and gas/wall thermochemistry characteristics for the above interior ballistics cases. This thermochemistry analysis interacts with the interior ballistics analysis (provides propellant properties, receives state variable ranges), boundary layer analysis (provides chemical composition, compressibility, and transport properties), and thermal/erosion analysis (provides inert wall enthalpies, reacting wall enthalpies, and blowing parameters). Validation of this code and product omissions are based on calibration with actual gas and gas/wall kinetic reaction rate data.

The MACE cannon code (refs 2,3) is based on a previous rocket code (ref 10) and calculates single-shot thermal and erosion characteristics, including wall temperature profiles and wall erosion profiles for the above interior ballistics cases. This thermal/erosion analysis interacts with the boundary layer analysis (receives adiabatic recovery enthalpies, cold wall heat transfer rates, and edge pressures), and thermochemistry analysis (receives inert wall enthalpies, reacting wall enthalpies, and blowing parameters). Validation of this code is based on its calibration with actual subsurface metallographic data (recrystallization, reaction, and transformation depths), thermocouple data, and borescope data.

RESULTS AND DISCUSSION

Figures 1 through 3 summarize the XNOVAKTC interior ballistics analysis for the four combinations of the 120-mm M256 cannon and its M865, M829, M829A1, and M829A2 KE round types. The M865 KE trainer round uses M14 propellant, while the M829Ax KE round series uses JA2 propellant. For these cannon-round type combinations, Figures 1 through 3 plot the respective maximum values of gas pressure (P_g), gas temperature (T_g), and gas velocity (V_g)

as a function of axial position and round-conditioning temperature. Although time-dependent data were calculated, maximum values were plotted instead of time-dependent data to simplify the appearance of these figures. Selected axial positions included 0.7, 1.6, 2.2, 3.3, and 5.1 meters from the RFT, while the selected round-conditioning temperatures included the hot (49°C), ambient (21°C), and cold (-32°C) conditions. These four round types, five selected axial positions, and three selected round-conditioning temperatures were used exclusively for the rest of the figures in this report. Experimental pressure-time and muzzle velocity data were used to calibrate these interior ballistics analyses. For the four respective round types above, the maximum T_g and P_g values decrease with increasing axial position, while the maximum V_g values increase with increasing axial position.

Figures 4 and 5 summarize the MABL analysis for the four combinations of the 120-mm M256 cannon and its M865, M829, M829A1, and M829A2 KE round types stated above. For these cannon-round type combinations, Figures 4 and 5 plot the respective maximum values of recovery enthalpy (H_r) and cold wall heat flux (Q_{cw}) as a function of axial position and round-conditioning temperature. Maximum values were again used instead of calculated time-dependent data to simplify the appearance of these figures. Experimental thermal recrystallization depth, reaction depth, transformation depth, and thermocouple data were used to calibrate this improved boundary layer analysis. The boundary layer heat transfer and enthalpy analysis included mass addition modifications, combustion case gas cooling modifications (1600°K gases), and turbulent heating modifications, which dramatically modified the core flow pattern given in the above interior ballistics analysis. For a given KE round type, subsurface metallographic data indicate that this initial 0.6 to 1.2 meter from RFT bore region has the highest T_g 's, highest P_g 's, deep cracks, and mild erosion due to significant combustion case gas cooling and mild turbulent heating of the bore surface in that region. For the same KE round type, subsurface metallographic data indicate that the subsequent 1.2 to 2.4 meter from RFT bore region has lower T_g 's, lower P_g 's, shallower cracks, and significantly increased erosion. This is due to diminished combustion case gas cooling and significantly increased turbulent heating of the bore surface in that region. For the four respective round types above, the maximum H_r and Q_{cw} values increase with increasing axial position for the 0.6 to 1.2 meter from RFT region, both values peak in the 1.2 to 2.4 meter range, and then both values decrease with increasing axial position to the muzzle.

Figure 6 summarizes the CCET thermochemical analysis for the four combinations of the 120-mm M256 cannon and its M865, M829, M829A1, and M829A2 KE round types also given above. For these cannon-round type combinations, Figure 6 plots the respective values of mean reacting wall enthalpy (H_w) and mean ablation potential (B_a) as a function of wall materials (high contraction (HC) chromium plate or A723 gun steel), propellant type, and wall temperature (T_{wall}). Experimental kinetic rate function data and subsurface metallographic data were used to calibrate the thermochemical analysis and transform the chemical equilibrium analysis into a partial chemical kinetic analysis. Characterization of crack wall layers, interfaced wall layers, bore surface layers, subsurface void residues, and surface residues further guided gas/wall kinetics calibration. For the four respective round types, the HC chromium maximum T_{wall} 's are about 1450°K, 1600°K, 1625°K, and 1650°K. These temperatures are all below their passivating oxidation temperature onset at about 2000°K, well below their metallic melting point at about

2130°K, and well below their oxide melting point at about 2540°K, thus explaining their inertness. Also, for the four respective round types, the A723/iron maximum T_{wall} 's are about 1300°K, 1350°K, 1375°K, and 1400°K. These temperatures are well above their rapid expansive flaking oxidation temperature onset at about 1055°K, below their iron oxide melting point at about 1640°K, and well below their A723/iron melting point at about 1720°K, thus explaining their reactivity.

Figure 7 summarizes the A723 subsurface exposure borescope analysis (through HC chromium plate cracks) for the four combinations of the 120-mm M256 cannon and its M865, M829, M829A1, and M829A2 KE round types. For these cannon-round type combinations, Figure 7 plots values of percent A723 subsurface exposure as a function of equivalent rounds fired and axial position. Since most cannons have a multiple-round type firing history, the equivalent rounds of each round type are calculated from that actual data. The actual data include round type, round count per round type, round-conditioning temperature per round type, and their overall order. This small sample of experimental borescope data is used to calibrate the erosion analysis. The four round types further consist of a varied distribution of hot, ambient, and cold temperature conditioning. Data collection involved the use of a magnifying borescope with a calibrated scale to measure the number and average area of each HC chromium platelet within a designated total area as a function of axial position for a given round count. For the 120-mm M256 cannon, the manufactured percent of A723 subsurface exposure nominally is about one percent due to fine cracks and finite shrinkage. For the four respective round types here, the percent of A723 subsurface exposure increases with increasing axial position for the 0.6 to 1.2 meter from RFT region, peaks in the 1.2 to 2.4 meter range, and then decreases with increasing axial position to the muzzle. Also, for the four respective round types, the percent of A723 subsurface initially rises rapidly then more slowly with increasing round count. The rapid rise region is due to HC chromium thermal recrystallization, nonmetallic out-gassing, and possibly compression resulting in its shrinkage and heat checking. The slower rise region is due to HC chromium platelet spalling. Mechanical muzzle wear is not considered in this report since this mechanism never erodes the region to condemnation.

Figures 8 through 10 summarize the MACE wall temperature (T_w) profile analysis for the four combinations of the 120-mm M256 cannon and its M865, M829, M829A1, and M829A2 KE round types. For these cannon-round type combinations, Figures 8 through 10 plot the respective maximum values of HC chromium surface temperature (convection), A723 interface temperature (convection and conduction at crack wall), and A723 surface temperature (convection) as a function of the selected axial positions and round-conditioning temperatures. Maximum values were again used instead of calculated time-dependent data to simplify the appearance of these figures. Experimental thermal recrystallization depth, reaction depth, transformation depth, and thermocouple data were used to calibrate this temperature profile analysis. Wall temperature profiles in Figures 8 through 10 follow the positional order of the heat transfer pattern from the boundary layer analysis in Figures 4 and 5. For the four respective round types above, the maximum T_w values increase with increasing axial position for the 0.6 to 1.2 meter from RFT region, both values peak in the 1.2 to 2.4 meter range, then both values decrease with increasing axial position to the muzzle. In addition, for the four respective round types, the HC chromium maximum T_w 's are about 1450°K, 1600°K, 1625°K, and 1650°K. These

temperatures are all below their passivating oxidation temperature onset at about 2000°K, well below their metallic melting point at about 2130°K, and well below their oxide melting point at about 2540°K, thus explaining their inertness. For the four respective round types, the A723 maximum interface T_w 's are about 1190°K, 1210°K, 1220°K, and 1230°K. These temperatures are well above their rapid expansive flaking oxidation temperature onset at about 1055°K, below their iron oxide melting point at about 1640°K, and well below their A723/iron melting point at about 1720°K, thus explaining their reactivity. Diffusion, reactions, transformations, and gas wash thermochemically degrade interfacial A723 at HC chromium plate heat-checked crack bases. Also, for the four respective round types, the A723 maximum T_w 's are about 1300°K, 1350°K, 1375°K, and 1400°K. These temperatures are well above their rapid expansive flaking oxidation temperature onset at about 1055°K, below their iron oxide melting point at about 1640°K, and well below their A723/iron melting point at about 1720°K, thus explaining their reactivity. Diffusion, reactions, transformations, and gas wash thermochemically degrade fully exposed surface A723 after HC chromium platelet spalling.

Figures 11 through 14 summarize the MACE rounds-to-wall erosion condemnation analysis for the four combinations of the 120-mm M256 cannon and its M865, M829, M829A1, and M829A2 KE round types. For these cannon-round type combinations, Figures 11 through 14 plot the respective values of rounds-to-erosion for round-conditioning temperatures of 49°C, 21°C, -32°C, and an equal distribution as a function of rounds-to-A723 gas wash onset (GWO, 0.127-mm), rounds-to-erosion condemnation (5-mm), and the selected axial positions. These two key erosion depth values were used instead of calculated erosion depth profile data to simplify the appearance of the figures. For Figures 11-14, rounds-to-wall erosion condemnation follow the positional order of the heat transfer pattern from the boundary layer analysis in Figures 4 and 5. For the four respective round types above, the rounds-to-erosion condemnation values decrease with increasing axial position for the 0.6 to 1.2 meter from RFT region. The values reach a minimum in the 1.2 to 2.4 meter range, where peak erosion occurs (2.2 meters for the purposes of this report), and then the values increase with increasing axial position to the muzzle.

For the four respective round types and their associated round-conditioning temperatures, peak erosion occurs at approximately the 2.2-meter position and rounds-to-erosion condemnation at that position governs cannon erosion life. Quantifying this 2.2-meter peak erosion position for the four respective round types, the 49°C rounds-to-gas wash onset occur at about 430, 150, 120, and 100, while the associated rounds-to-erosion condemnation occur at about 1430, 510, 430, and 340. Quantifying this 2.2-meter peak erosion position for the four respective round types, the 21°C rounds-to-gas wash onset occur at about 640, 220, 180, and 150, while the associated rounds-to-erosion condemnation occur at about 2150, 770, 640, and 510. Quantifying this 2.2-meter peak erosion position for the four respective round types, the -32°C rounds-to-gas wash onset occur at about 970, 330, 270, and 220, while the associated rounds-to-erosion condemnation occur at about 3220, 1150, 960, and 770. Quantifying this 2.2-meter peak erosion position for the four respective round types, the equal distribution of 49°C, 21°C, and -32°C rounds-to-gas wash onset occur at about 610, 210, 170, and 140, while the associated rounds-to-erosion condemnation occur at about 2030, 730, 610, and 490.

Figure 15 summarizes the MACE erosion EFC analysis for the four combinations of the 120-mm M256 cannon and its M865, M829, M829A1, and M829A2 KE round types. For these cannon-round type combinations, Figure 15 plots the erosion EFC factors (or values) as a function of round type and round-conditioning temperature. These erosion EFC factors are based on an erosion EFC factor of 1.0 for the M865 round type at a 21°C round-conditioning temperature as requested by PM-TMAS (Picatinny Arsenal, NJ), and these erosion factors correspond to a peak erosion location of approximately 2.2 meters from the RFT. For the M256 cannon and the M865, M829, M829A1, and M829A2 round types at a 49°C round-conditioning temperature, the respective erosion EFC factors are approximately 1.5, 4.2, 5.0, and 6.3. Similarly, the respective erosion EFC factors are approximately 1.0, 2.8, 3.3, and 4.2 at a 21°C round conditioning temperature; they are approximately 0.7, 1.9, 2.2, and 2.8 at a -32°C round-conditioning temperature; and they are approximately 1.1, 3.0, 3.5, and 4.4 for an equal distribution of these three round-conditioning temperatures.

For the above cannon and round combinations, the main cannon erosion mechanism consists of nonequilibrium chromium plate and gun steel degradation (cracking, shrinkage by thermal recrystallization/out-gassing, crack widening, and heat checking). This is followed by degradation of the subsurface gun steel substrate at radial crack walls (diffusion, reactions, transformations, and gas wash), subsequent gun steel degradation link-up coupled with mild shear forces causing chromium platelet spalling, and subsequent bare gun steel gas wash (refs 2,3). For a given KE round used in the M256 cannon, the following factors have been measured as a function of axial position and cumulative rounds fired (ref 3): resultant crack depths chromium recrystallization depths, chromium out-gassing products, crack widths, carbon/gun steel diffusion products, oxygen/gun steel reaction products, oxygen/chromium reaction products, gun steel transformation depths, and gun steel gas wash depths.

The U.S. Army and Air Force's standard manual for the evaluation of cannon tubes designates fatigue condemnation criteria for each cannon tube type. It also designates erosion condemnation criteria for each cannon tube type and designates a cartridge/zone fatigue EFC factor for each charge/projectile combination. This helps manage cannon inventory. However, the manual lacks a designated cartridge/zone erosion EFC factor for each charge/projectile combination, thus representing a notable technology gap for tank and artillery cannon systems, since erosion condemnation occurs much quicker than fatigue condemnation when using the latest charge/projectile combinations. Our report has outlined a detailed computational and experimental method using the Unified Cannon Erosion Code and related experimental data for computing a cartridge or round erosion EFC factor for the M865, M829, M829A1, and M829A2 KE round types used in the 120-mm M256 tank cannon at multiple round-conditioning temperatures. Our report has further outlined the obvious extension of this method to any group of charge/projectile combinations used in a specific tank or artillery cannon. These round type and conditioning temperature-dependent erosion EFC factors, in combination with the designated erosion condemnation depth, further help the Army manage its M256 cannon inventory.

REFERENCES

1. *Evaluation of Cannon Tubes*, Headquarters Department of Army Technical Manual TM-9-1000-202-14 and Headquarters Department of Air Force Technical Order TO-11W2-17-5-1, Washington, DC, June 1993.
2. Dunn, S., Sopok, S., Coats, D., O'Hara, P., Nickerson, G., and Pflegl, G., "Unified Computer Model for Predicting Thermochemical Erosion in Gun Barrels," *Proceedings of 31st AIAA Joint Propulsion Conference*, San Diego, CA, July 1995.
3. Sopok, S., Vottis, P., O'Hara, P., Pflegl, G., and Rickard, C., "Shot-by-Shot Erosion Modeling of Retired 120-mm M256 Gun Tube #1988," *Proceedings of 34th AIAA Joint Propulsion Conference*, Cleveland, OH, July 1998.
4. Gough, P., "The XNOVAKTC Code," Paul Gough Associates, Portsmouth NH, U.S. Army BRL-CR-627, February 1990.
5. Levine, J., "Transpiration and Film Cooling Boundary Layer Computer Program (MABL) - Numerical Solution of the Turbulent Boundary Layer Equations with Equilibrium Chemistry," NASA Marshall N72-19312, June 1971.
6. Nickerson, G., Berker, D., Coats, D., and Dunn, S., "Two-Dimensional Kinetics (TDK) Nozzle Performance Computer Program," Software and Engineering Associates, Inc., Carson City, NV, NASA Marshall NAS8-39048, March 1993.
7. Coats, D., and Dunn, S., "A New Chemical Equilibrium Code with Compressibility Effects," *Proceedings of the 33rd JANNAF Combustion Meeting*, Monterey, CA, October 1996.
8. Gordon, S., and McBride, B., "Computer Program for Calculation of Complex Chemical Equilibrium Compositions, Rocket Performance, Incident and Reflected Shocks, and Chapman-Jouguet Detonations (CET)," NASA SP-273, NASA Lewis Research Center, Cleveland, OH, March 1971.
9. Freedman, E., "BLAKE - A Thermodynamic Code Based on Tiger: User's Guide and Manual," Technical Report ARBRL-TR-02411, U.S. Army Ballistic Research Laboratory, Aberdeen Proving Ground, MD, July 1982.
10. Dunn, S., "Materials Ablation Conduction Erosion Program (MACE)," Software and Engineering Associates, Inc., Carson City, NV, June 1989.

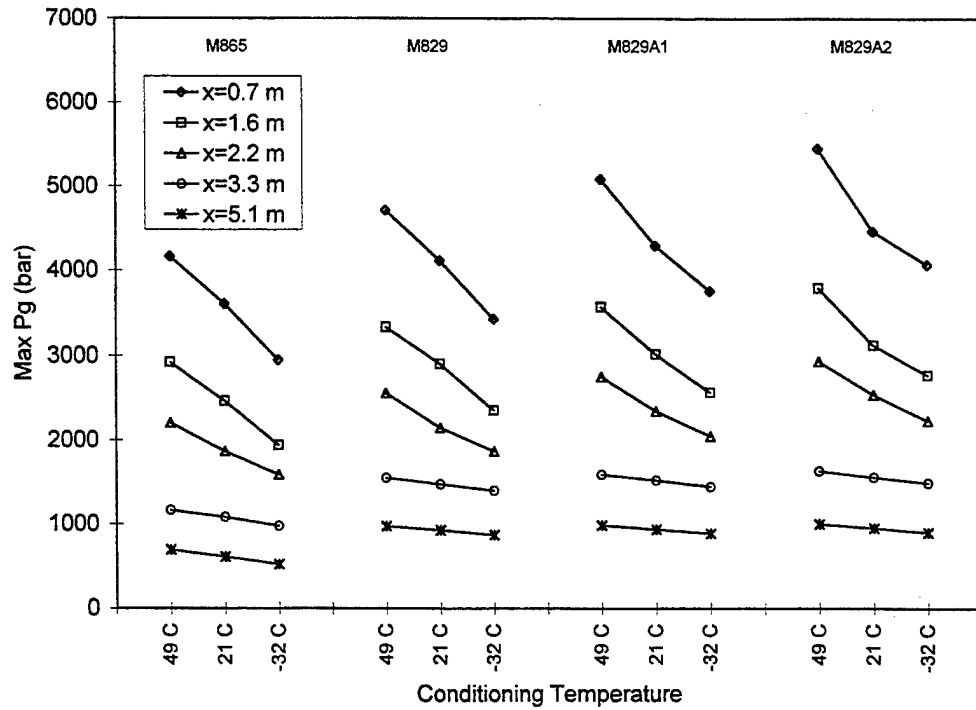


Figure 1. M256 calibrated XNOVAKTC interior ballistics analysis for maximum values of gas pressure.

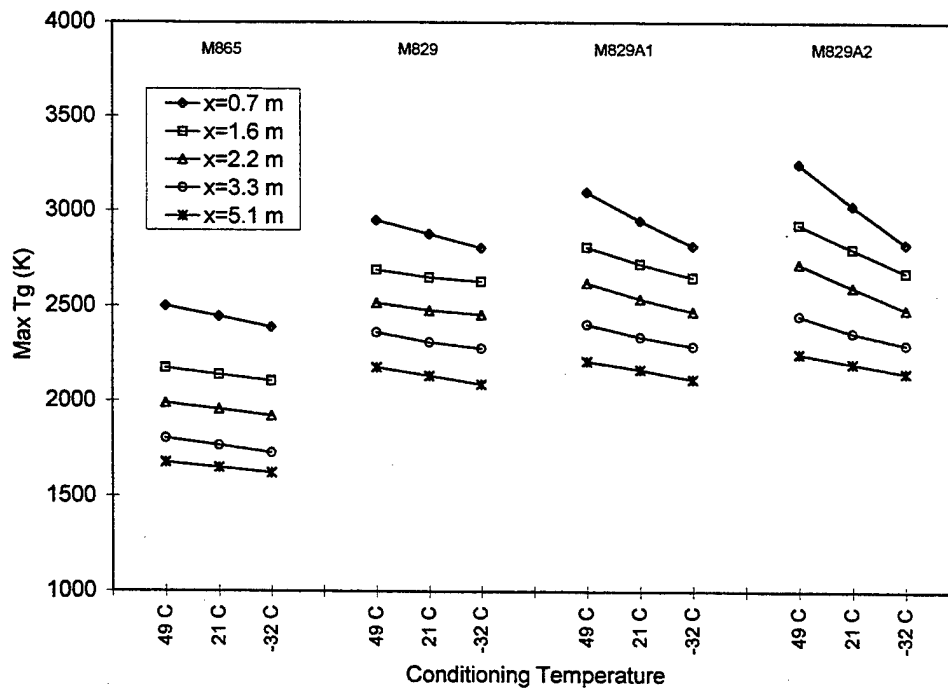


Figure 2. M256 calibrated XNOVAKTC interior ballistics analysis for maximum values of gas temperature.

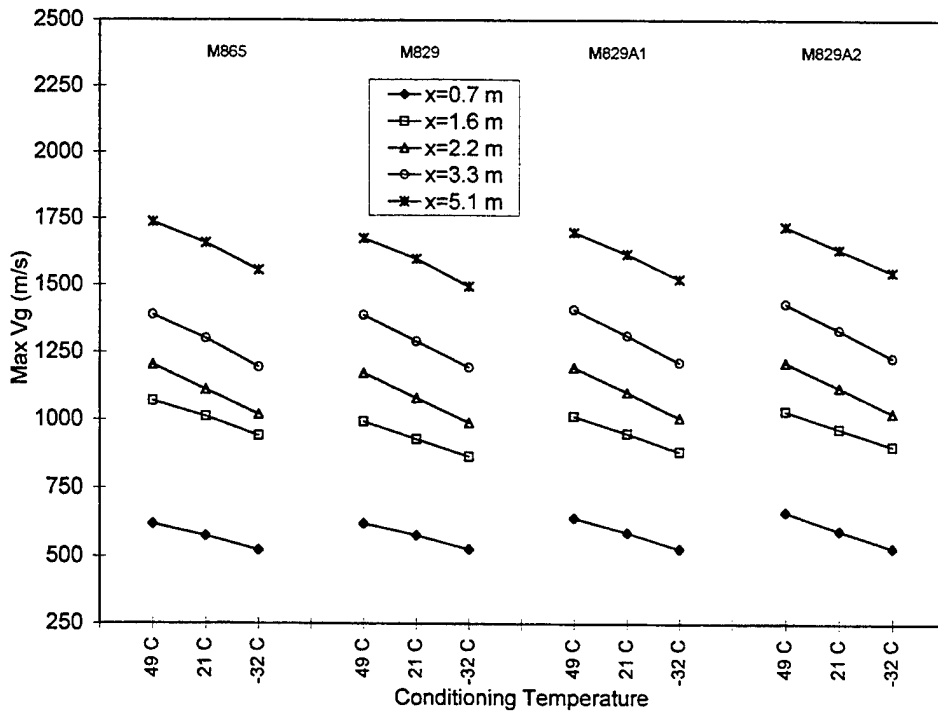


Figure 3. M256 calibrated XNOVAKTC interior ballistics analysis for maximum values of gas velocity.

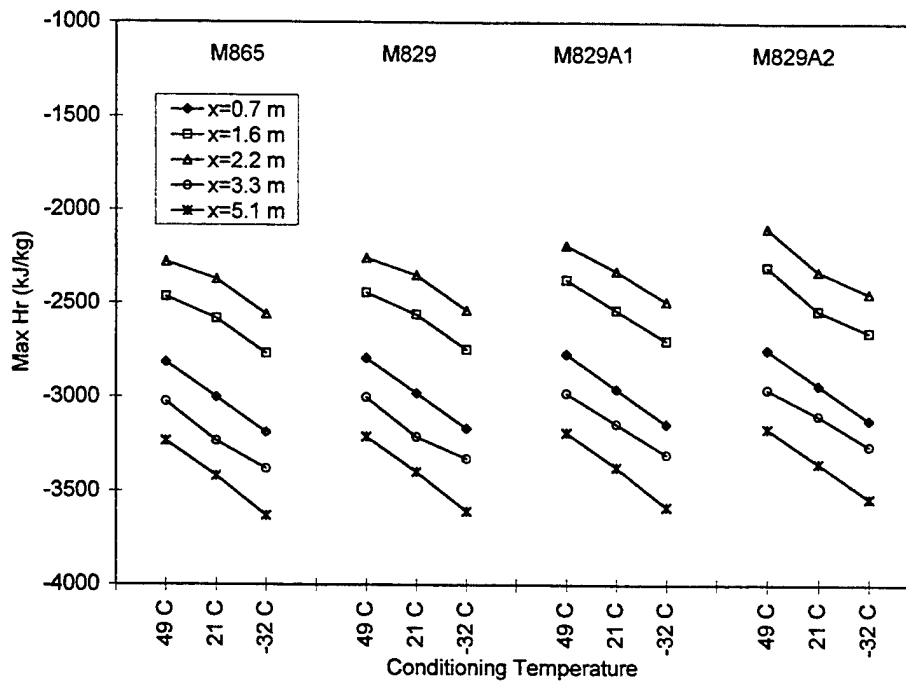


Figure 4. M256 calibrated MABL analysis for maximum values of recovery enthalpy.

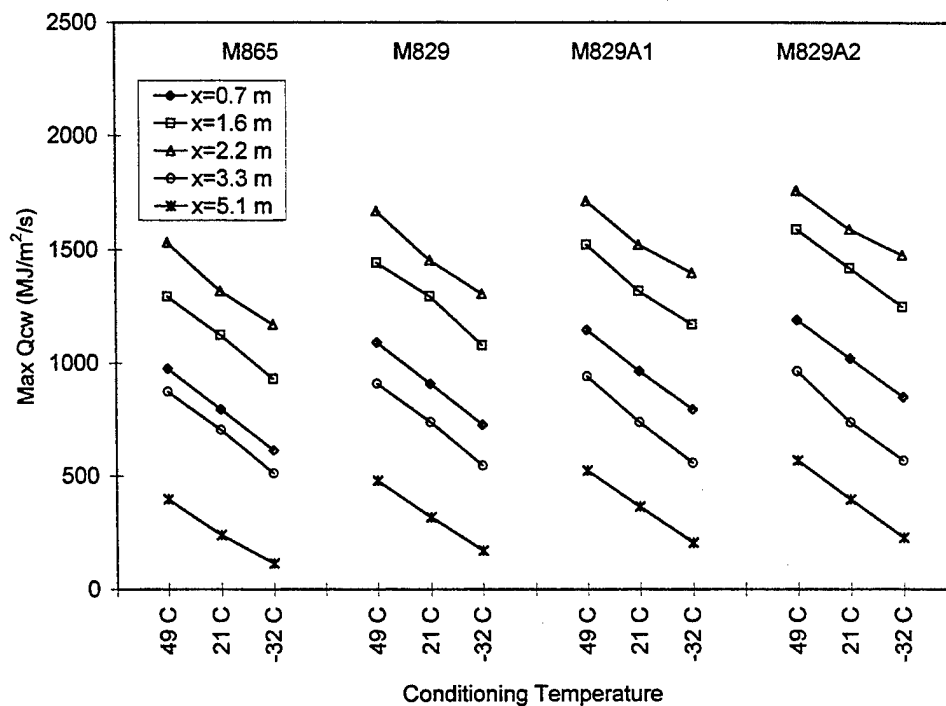


Figure 5. M256 calibrated MABL analysis for maximum values of cold wall heat flux.

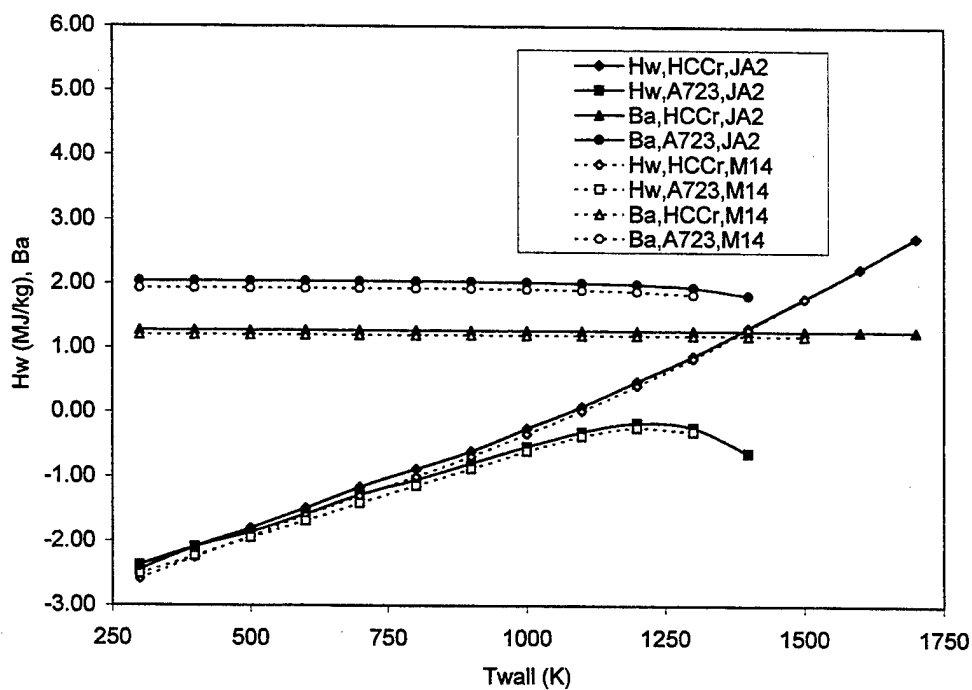


Figure 6. M256 calibrated CCET thermochemical analysis for respective values of mean reacting wall enthalpy and mean ablation potential.

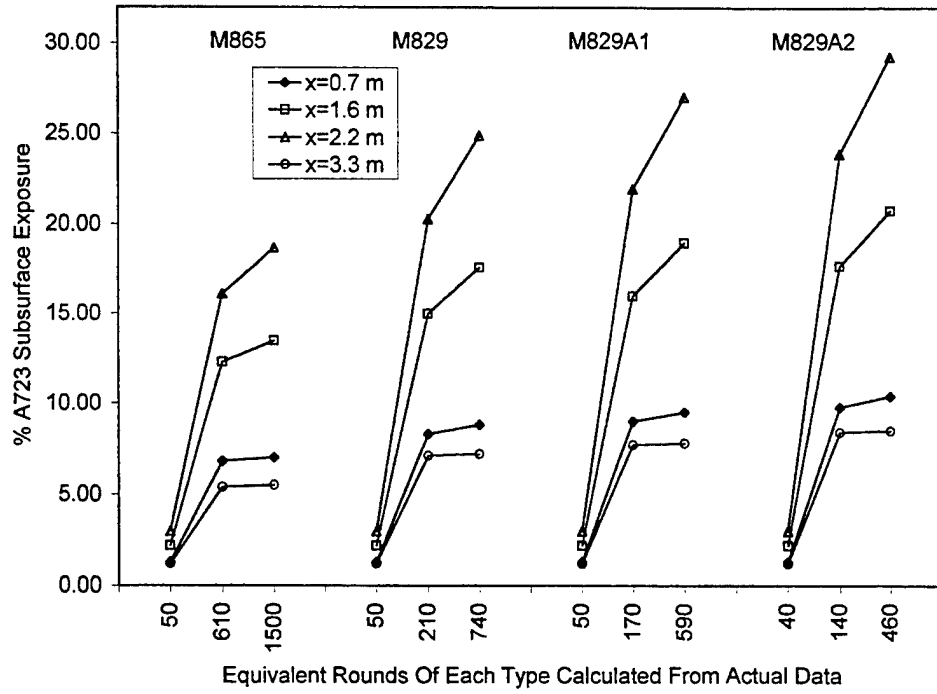


Figure 7. Borescope analysis of the A723 subsurface exposure.

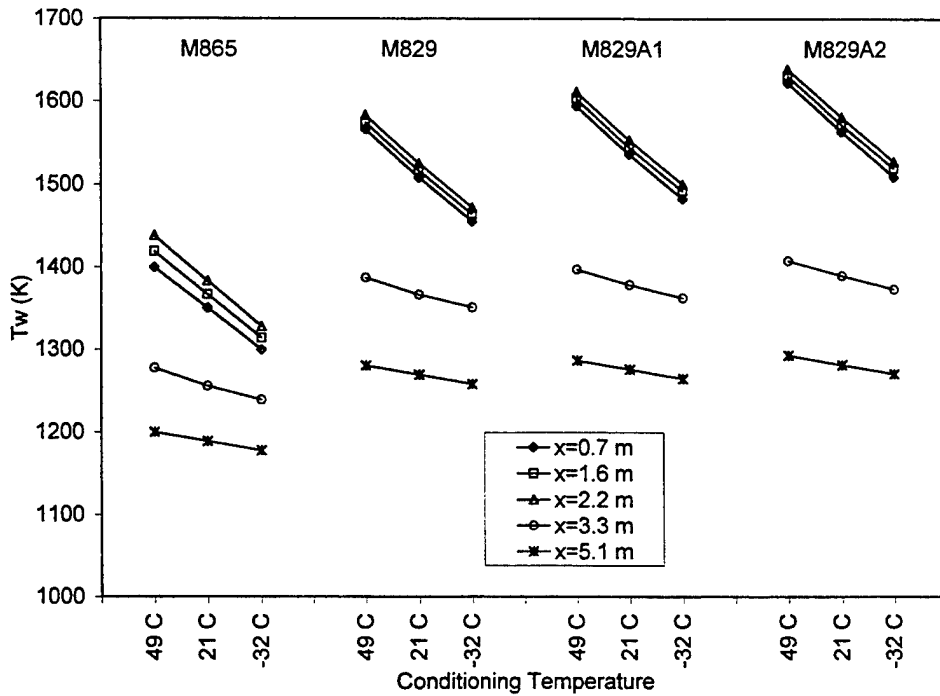


Figure 8. M256 calibrated MACE wall temperature profile analysis for maximum values of HC chromium surface temperature.

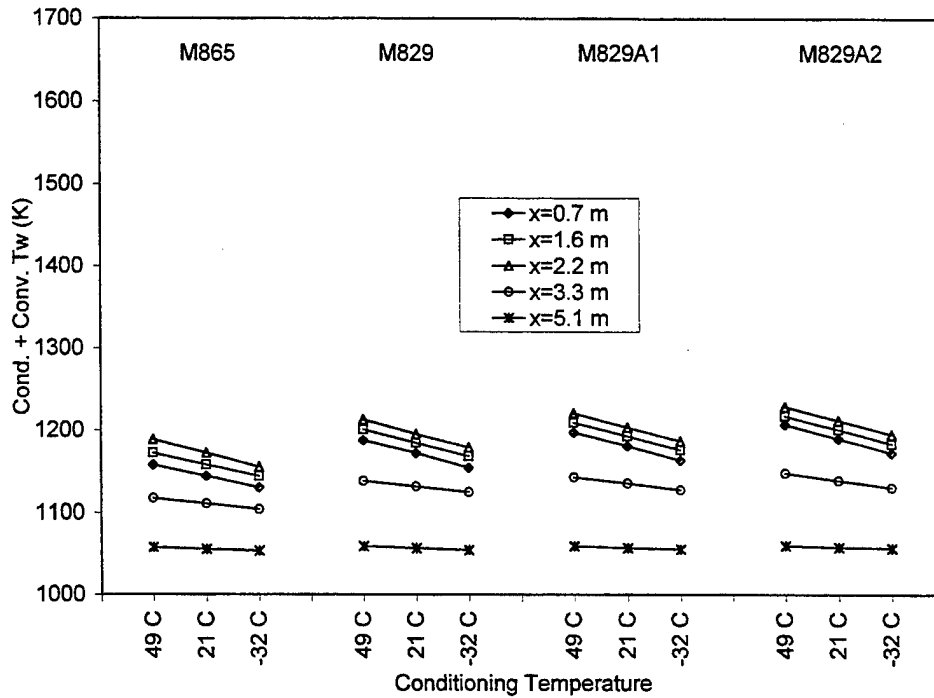


Figure 9. M256 calibrated MACE wall temperature profile analysis for maximum values of A723 interface temperature.

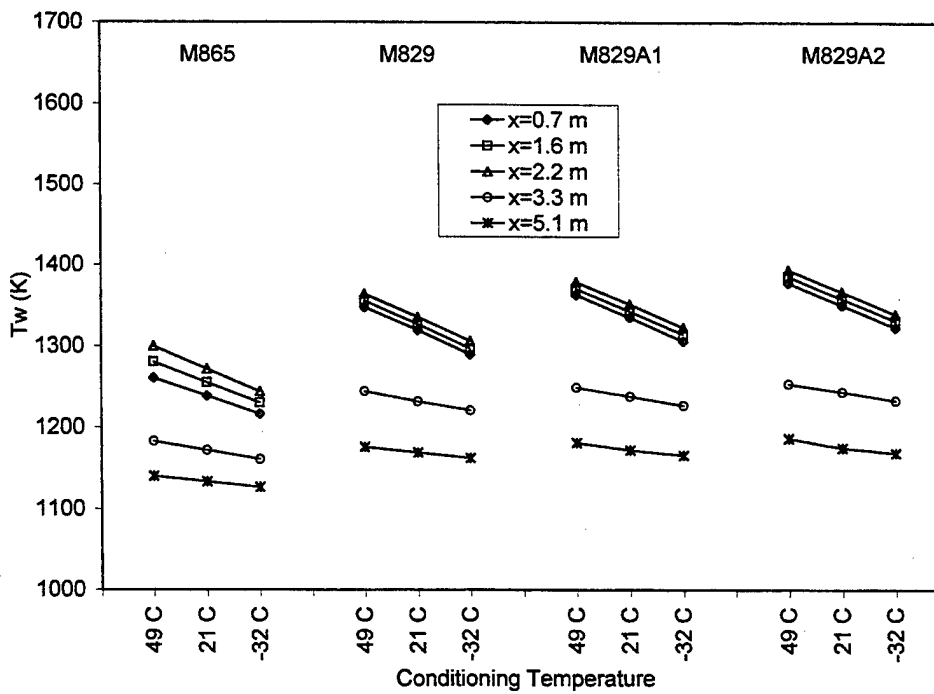


Figure 10. M256 calibrated MACE wall temperature profile analysis for maximum values of A723 surface temperature.

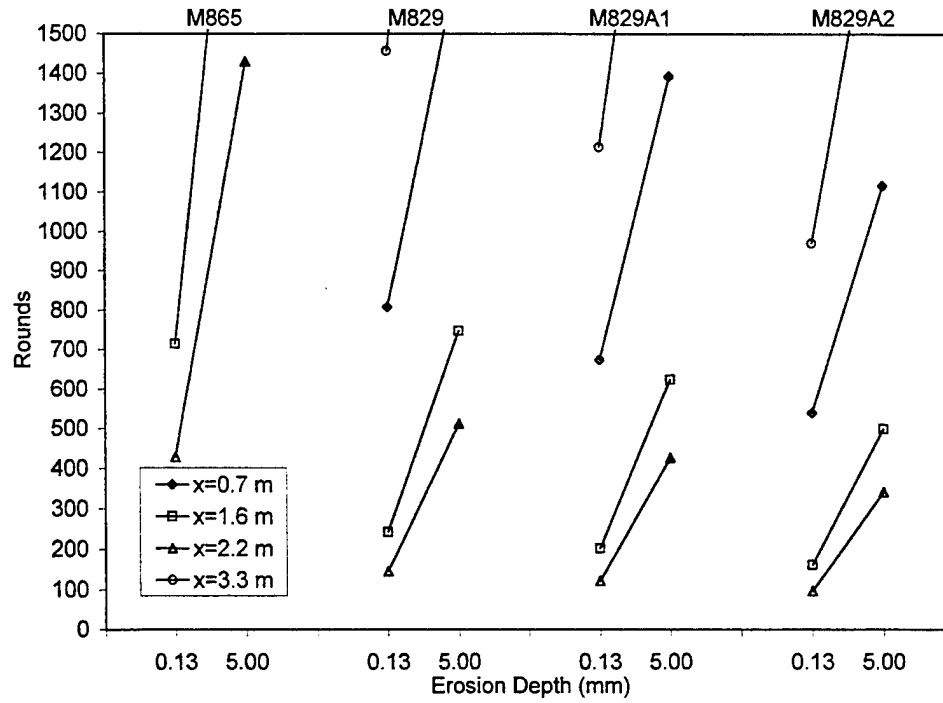


Figure 11. M256 MACE analysis of rounds-to-gas wash onset and rounds-to-erosion condemnation for round-conditioning temperature of 49°C.

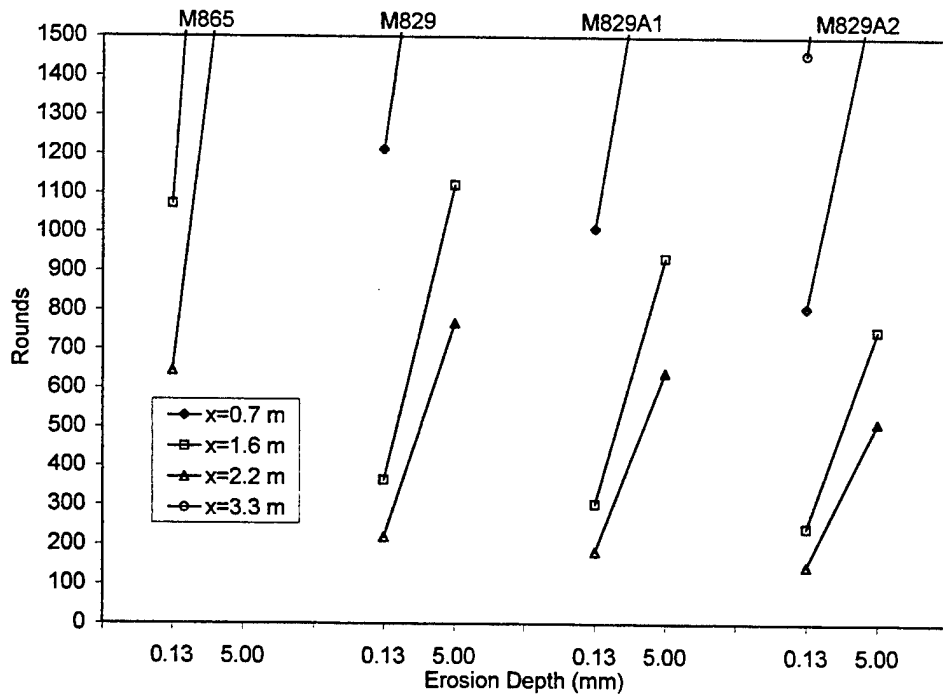


Figure 12. M256 MACE analysis of rounds-to-gas wash onset and rounds-to-erosion condemnation for round-conditioning temperature of 21°C.

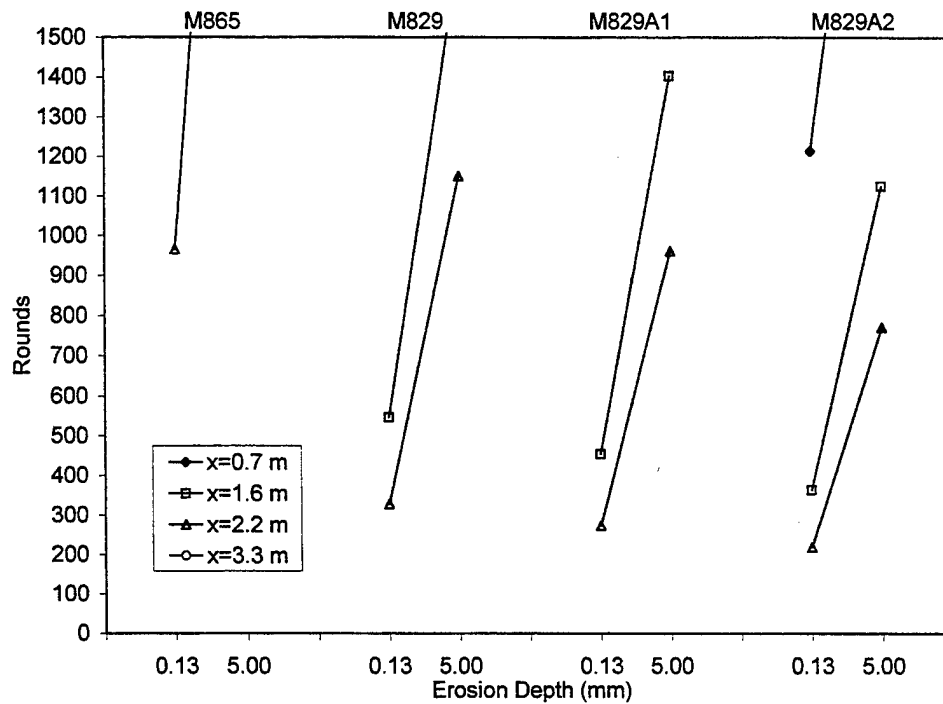


Figure 13. M256 MACE analysis of rounds-to-gas wash onset and rounds-to-erosion condemnation for round-conditioning temperature of -32°C.

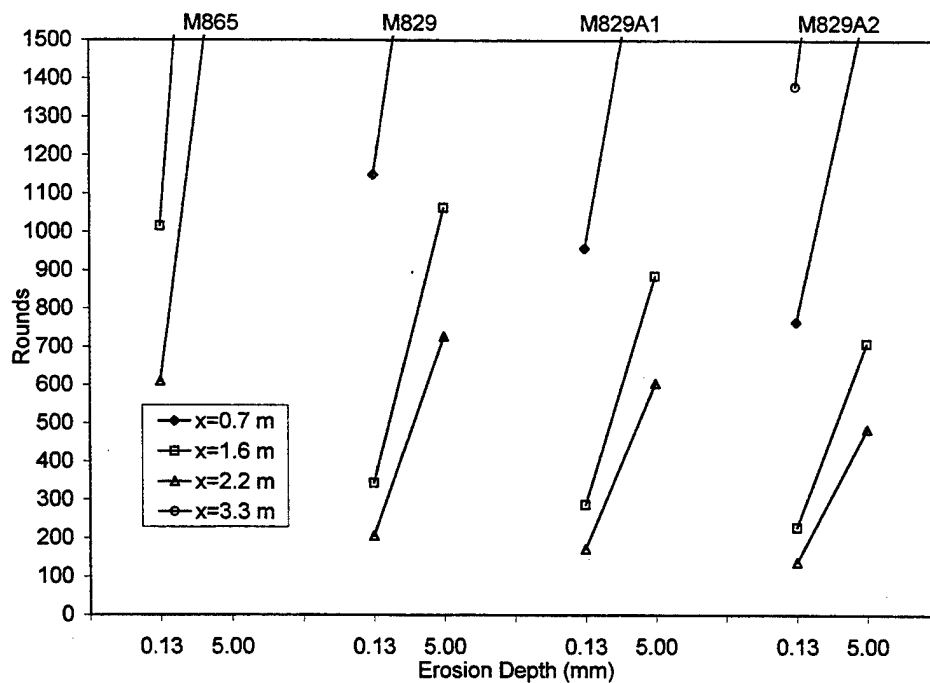


Figure 14. M256 MACE analysis of rounds-to-gas wash onset and rounds-to-erosion condemnation for an equal distribution of 49°C, 21°C, and -32°C.

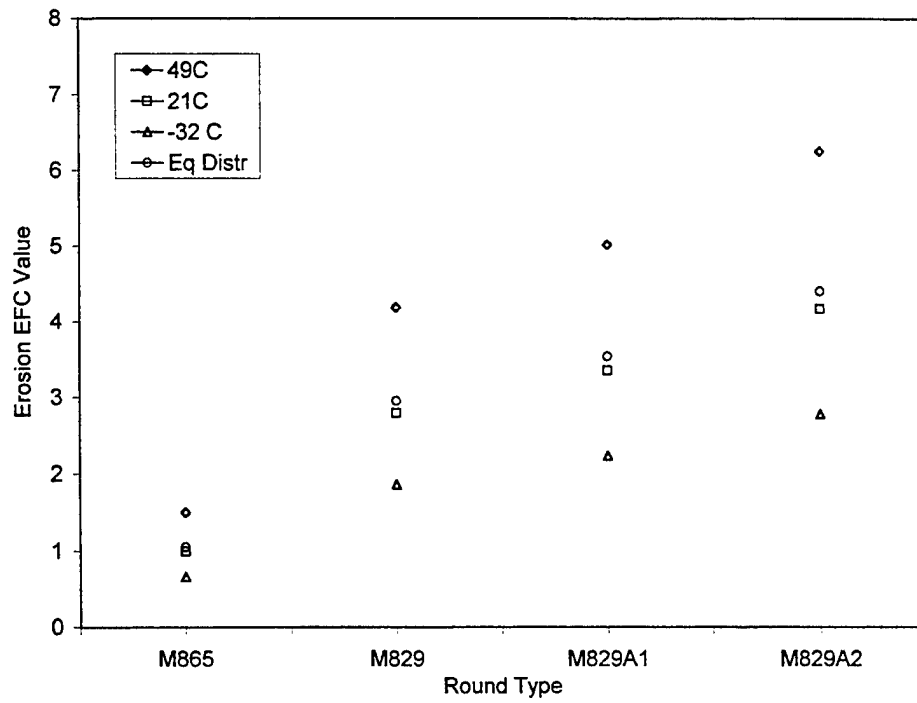


Figure 15. M256 MACE erosion EFC analysis based on an erosion EFC factor of 1.0 for the M865 round type at 21°C round-conditioning temperature.

TECHNICAL REPORT INTERNAL DISTRIBUTION LIST

	<u>NO. OF COPIES</u>
TECHNICAL LIBRARY ATTN: AMSTA-AR-CCB-O	5
TECHNICAL PUBLICATIONS & EDITING SECTION ATTN: AMSTA-AR-CCB-O	3
OPERATIONS DIRECTORATE ATTN: SIOWV-ODP-P	1
DIRECTOR, PROCUREMENT & CONTRACTING DIRECTORATE ATTN: SIOWV-PP	1
DIRECTOR, PRODUCT ASSURANCE & TEST DIRECTORATE ATTN: SIOWV-QA	1

NOTE: PLEASE NOTIFY DIRECTOR, BENÉT LABORATORIES, ATTN: AMSTA-AR-CCB-O OF ADDRESS CHANGES.

TECHNICAL REPORT EXTERNAL DISTRIBUTION LIST

	<u>NO. OF COPIES</u>		<u>NO. OF COPIES</u>
DEFENSE TECHNICAL INFO CENTER		COMMANDER	
ATTN: DTIC-OCA (ACQUISITIONS)	2	ROCK ISLAND ARSENAL	
8725 JOHN J. KINGMAN ROAD		ATTN: SIORI-SEM-L	1
STE 0944		ROCK ISLAND, IL 61299-5001	
FT. BELVOIR, VA 22060-6218			
COMMANDER		COMMANDER	
U.S. ARMY ARDEC		U.S. ARMY TANK-AUTMV R&D COMMAND	
ATTN: AMSTA-AR-WEE, BLDG. 3022	1	ATTN: AMSTA-DDL (TECH LIBRARY)	1
AMSTA-AR-AET-O, BLDG. 183	1	WARREN, MI 48397-5000	
AMSTA-AR-FSA, BLDG. 61	1	COMMANDER	
AMSTA-AR-FSX	1	U.S. MILITARY ACADEMY	
AMSTA-AR-FSA-M, BLDG. 61 SO	1	ATTN: DEPT OF CIVIL & MECH ENGR	1
AMSTA-AR-WEL-TL, BLDG. 59	2	WEST POINT, NY 10966-1792	
PICATINNY ARSENAL, NJ 07806-5000			
DIRECTOR		U.S. ARMY AVIATION AND MISSILE COM	
U.S. ARMY RESEARCH LABORATORY		REDSTONE SCIENTIFIC INFO CENTER	2
ATTN: AMSRL-DD-T, BLDG. 305	1	ATTN: AMSAM-RD-OB-R (DOCUMENTS)	
ABERDEEN PROVING GROUND, MD		REDSTONE ARSENAL, AL 35898-5000	
21005-5066			
DIRECTOR		COMMANDER	
U.S. ARMY RESEARCH LABORATORY		U.S. ARMY FOREIGN SCI & TECH CENTER	
ATTN: AMSRL-WM-MB (DR. B. BURNS)	1	ATTN: DRXST-SD	1
ABERDEEN PROVING GROUND, MD		220 7TH STREET, N.E.	
21005-5066		CHARLOTTESVILLE, VA 22901	
COMMANDER			
U.S. ARMY RESEARCH OFFICE			
ATTN: TECHNICAL LIBRARIAN	1		
P.O. BOX 12211			
4300 S. MIAMI BOULEVARD			
RESEARCH TRIANGLE PARK, NC 27709-2211			

NOTE: PLEASE NOTIFY COMMANDER, ARMAMENT RESEARCH, DEVELOPMENT, AND ENGINEERING CENTER,
 BENÉT LABORATORIES, CCAC, U.S. ARMY TANK-AUTOMOTIVE AND ARMAMENTS COMMAND,
 AMSTA-AR-CCB-O, WATERVLIET, NY 12189-4050 OF ADDRESS CHANGES.
